1983/15. Petrology of contact metamorphosed Mathinna Beds, near Trigonia Corner, Maria Island.

J.L. Everard

Abstract

East of Trigonia Corner, south Maria Island, Mathinna Beds psammites are intruded and contact metamorphosed by Devonian-Carboniferous granite. Fifty metres from the contact, the assemblage muscovite-chlorite-K feldspar-albite-quartz is merely that of the very low-grade regional metamorphism that pervades the Mathinna Beds, although there is some textural evidence for thermally induced recrystallisation. A few centimetres from the contact the assemblage is phengitic muscovite-biotite-K feldspar-albite-quartz. The narrowness of the aureole and the absence of cordierite at the contact, despite an appropriate bulk composition, suggest unusually weak contact metamorphism. Assuming that $P_{H_2O} \cong P_{total} = 1$ to 2.5 kb, the temperature at the contact probably did not exceed 500° to 600°C. The most probable explanation seems to be that the granite intruded at relatively low temperatures.

INTRODUCTION

During regional mapping of the Maria Quadrangle, P.W. Baillie mapped an area of contact metamorphic Siluro-Devonian Mathinna Beds psammite and spotted pelite, intruded by Devonian-Carboniferous porphyritic, fine to medium-grained granite, to the east of Trigonia Corner, Maria Island. Baillie collected two samples of hornfels from the foreshore near EN886733, one (MA18) about 50 m from the contact and another (MA19) from within a few centimetres of the contact. Polished thin sections were prepared and studied with the optical microscope, and the electron probe microanalyser at the University of Tasmania, in an effort to determine the metamorphic grade and possibly the physical conditions prevailing during intrusion of the granite.

PETROGRAPHY

MA18

This rock is a rather poorly sorted, weakly recrystallised psammite consisting of (n = 200) quartz (61%), orthoclase and albite (9%), intergranular muscovite (21%) and chlorite (8%), and accessory (1%) tourmaline, zircon, ?rutile and altered ilmenite (leucoxene).

Interlocking, equant anhedra of quartz (mostly 30-300 μm) and subordinate, equant to irregular anhedra of feldspar (typically 40-200 μm) comprise most of the rock. Feldspar is distinguished optically from quartz by a cloudy to finely mottled appearance due to incipient to partial sericitisation, and electron probe microanalysis suggests that orthoclase is somewhat more abundant than albite. The frequent interlocking of quartz and feldspar grains and the unstrained nature of the quartz (unlike much quartz from Mathinna Bed rocks) suggest that thermal metamorphism has caused some recrystallisation, possibly driven by the release of lattice strain of quartz, acquired during regional deformation and very low-grade regional metamorphism. However, curved to irregular grain boundaries and very unequal grain sizes indicate that equilibrium texture was not attained.

Muscovite and chlorite both occur as small (20-150 μm long), very

ragged laths, splinters and irregular subhedral to anhedral fragments, lying between or interstitial to quartz and feldspar grains. There is a strong preferred orientation of the laths, probably corresponding to macroscopic cleavage. Muscovite and chlorite are often intergrown on a macroscopic scale with apparent crystallographic alignment, but usually occur separately. Muscovite is colourless, with high birefringence and a higher relief when orientated with cleavage parallel to the nicol; electron probe microanalyses (Table 1) show the muscovite to be somewhat phengitic, with a high silica content and about 3 mol% trioctahedral component. Chlorite, which is pale yellow-green and almost isotropic, sometimes with anomalous berlin-blue birefringence, is a ferroan ripidolite (Table 1) after the nomenclature of Hey (1954).

Accessory minerals include tiny (5-15 μm) rounded to ovate, cleavageless blebs of pleochroic, pale yellowish to orange-brown tourmaline; small (10-30 μm) elongate euhedral to rounded zircons; and very deep red to almost opaque ?rutile. Sparsely distributed, angular to irregular opaque material (rarely 200 μm, to dust) consists, according to probe analyses, of ilmenite now largely altered to titanium oxide ('leucoxene'). These minerals are probably all of detrital origin and have been reported in unmetamorphosed Mathinna Beds (*e.g.* Turner *in* McClenaghan *et al.*, 1982, p.14; Marshall, 1970, p.19).

MA19

This is a granoblastic-polygonal quartz-feldspathic hornfels, differing from MA18 in not only being finer grained and less quartz-rich, but in showing more mineralogical and textural evidence of contact metamorphism. It consists of (n = 200) quartz (25%), albite and orthoclase (43%), biotite (28%) and muscovite, with accessory (1%) tourmaline, zircon and altered ilmenite. Biotite laths have a fairly well-developed preferred orientation, which could correspond either to regionally developed cleavage, or cleavage caused by stress associated with emplacement of the granite (*cf.* Marshall, 1970, p.71).

Quartz occurs as large (up to 400 μm), isolated equant anhedra, ranging to much smaller (≧30 μm) interlocking equant polygonal to irregular anhedra, often associated with similar (20-700 μm) polygonal anhedra of incipiently to partially sericitised alkali feldspar. Electron probe microanalyses suggest that albite is somewhat more abundant than orthoclase. This interlocking quartz-feldspathic groundmass is somewhat more equidimensional, and with straighter grain boundaries, than in MA18, but nevertheless the even-grained polygonal equilibrium texture for quartzites (*cf.* Spry, 1969, p.188) has not been attained.

Short (30-100 μm) stubby laths of biotite are abundant throughout the slide. Biotite is pleochroic from deep red-brown ($\beta=\gamma$) to nearly colourless (α), and basal sections give a virtually uniaxial negative interference figure. Electron probe microanalyses show a siderophyllite-like composition, with Fe/Fe+Mg=0.50-0.57 and appreciable aluminium in the octahedral sites (Table 2). Biotite is sometimes partly or wholly altered to a pale-greenish, length-slow, low birefringence brunsvigitic chlorite (Table 2, analysis H).

Muscovite occurs as occasional ragged, colourless, high-birefringence laths of similar size to those of chlorite, or colourless low-birefringence anhedral basal sections with a biaxial negative interference figure. Although less abundant than biotite, muscovite is well crystallised and is clearly prograde. Electron probe microanalyses (Table 2), show that the

Table 1. ANALYSES OF MINERALS, SAMPLE MA18

	Muscovites			Chlorites			
	A	B	C	D	E	F	G
SiO_2	47.27	47.85	46.53	24.68	23.85	25.09	25.10
Al_2O_3	36.24	36.45	36.30	20.84	19.32	22.35	21.46
FeO	0.98	0.69	0.79	27.16	28.43	27.41	29.04
MgO	0.52	0.59	0.42	11.58	10.46	13.75	13.09
Na_2O	0.32	0.45	0.47	-	-	-	-
K_2O	10.14	10.33	10.40	-	-	-	-
Total	95.46	96.35	94.91	84.27	82.07	88.60	88.70
H_2O(by diff.)	4.54	3.65	5.09	15.73	17.93	11.40	11.30
Structural Formulae							
	No. of ions assuming (O)=11			No. of ions assuming (O)=14, Z=10			
Si	3.114	3.122	3.091	2.766	2.773	2.645	2.665
Al^{iv}	0.886	0.878	0.909	1.234	1.227	1.355	1.335
Al^{vi}	1.928	1.925	1.933	1.519	1.422	1.422	1.350
Fe	0.054	0.038	0.044	2.546	2.765	2.417	2.578
Mg	0.051	0.058	0.042	1.935	1.813	2.161	2.072
K	0.851	0.860	0.881	-	-	-	-
Na	0.041	0.057	0.061	-	-	-	-
Fe/Fe+Mg				0.626	0.604	0.528	0.554

All analyses were obtained using a JEOL JX-50A electron probe microanalyser at the Central Science Laboratory, University of Tasmania. The 'spot' mode (beam diameter <0.5 μm, penetration 3-5 μm) was used. Oxides sought but not found include TiO_2, Cr_2O_3, MnO, and CaO. Analyses have been converted to structural formulae assuming all iron is in the divalent state and an ideal content of (O) and (OH).

Table 2. ANALYSES OF MINERALS, SAMPLE MA19

	Muscovites			Biotites				Secondary chlorite
	A	B	C	D	E	F	G	H
SiO_2	45.86	46.50	46.22	38.35	36.54	39.17	35.68	24.26
TiO_2	0.40	-	0.26	1.88	2.76	2.19	1.73	-
Al_2O_3	29.76	35.70	32.31	19.84	18.08	19.11	19.14	20.86
FeO	1.94	1.90	3.35	17.50	19.26	16.85	23.00	33.27
MgO	1.51	-	1.23	9.81	8.37	8.07	6.97	6.33
CaO	-	-	0.63	-	-	-	0.40	-
Na_2O	-	-	0.42	0.50	-	-	-	-
K_2O	9.78	11.40	11.14	8.24	9.40	8.50	9.17	-
Total	89.25	95.50	95.56	96.12*	94.41	93.89	95.87	84.73
H_2O (by diff.)	10.75	4.50	4.44	3.88*	5.59	6.11	4.13	15.27
Structural Formulae								
Si	3.253	3.100	3.123	2.820	2.796	2.932	2.731	2.818
Al^{iv}	0.747	0.900	0.877	1.180	1.204	1.068	1.269	1.182
Al^{vi}	1.742	1.906	1.697	0.540	0.426	0.619	0.458	1.674
Ti	0.022	-	0.013	0.104	0.159	0.124	0.100	-
Fe	0.116	0.106	0.189	1.077	1.233	1.055	1.472	3.231
Mg	0.160	-	0.124	1.075	0.955	0.900	0.795	1.095
Ca	-	-	0.045	-	-	-	0.033	-
K	0.885	0.970	0.960	0.773	0.918	0.812	0.896	-
Na	-	-	0.055	0.071	-	-	-	-
Fe/Fe+Mg				0.501	0.564	0.540	0.649	0.747

* recalculated to ideal H_2O^+

Analyses obtained and treated as for MA18 (Table 1).

muscovite is a silica-rich phengitic variety chemically similar to that of MA18, although with a greater trioctahedral component (about 10 mol%).

Accessory minerals of probable detrital origin include, as in MA18, small (≤100 μm), elongate, rounded zircons, possibly orange-brown blebs of tourmaline, and rounded to irregular or hexagonal equant opaque blebs which analysis shows to be, as before, altered ilmenite (leucoxene).

Despite a careful search, both optically and with the electron probe, no cordierite or altered cordierite was found.

BULK COMPOSITION

Whole rock analysis was not considered warranted and in any case little material remained after sectioning. However, two estimates of the bulk composition of each sample were made (Table 3), firstly using a broad area (1 mm x 700 μm) scan on the electron probe microanalyser, and secondly by estimating the mode by point counting (n = 200) and converting this to a bulk composition using, where necessary, average mineral compositions obtained by electron probe microanalysis (Tables 1, 2). Given the errors and approximations involved, the estimates agree reasonably well.

Table 3. ESTIMATED BULK COMPOSITION OF SAMPLES

	MA18		MA19	
	Scan	Mode	Scan	Mode
SiO_2	83.87	77.5	62.00	65.4
TiO_2	-	1.5	0.63	0.7
Al_2O_3	8.02	11.4	19.06	14.9
FeO	3.00	2.8	5.10	6.2
MgO	1.09	1.2	1.60	2.6
CaO	-	-	0.33	0.04
Na_2O	0.57	0.5	4.33	3.23
K_2O	2.34	3.1	6.94	5.53
H_2O^+	1.12*	2.0	7.19*	1.4
Total	100.00	100.0	100.00	100.0

* by difference

PHASE RELATIONS

As both samples contain negligible CaO and excess quartz, their mineralogy can, as outlined by Winkler (1979, p.39-44), be represented by A'FK diagrams, with quartz and albite as additional phases (fig. 1).

Despite a field appearance of hornfels, the assemblage of MA18 (muscovite-chlorite-K feldspar-albite-quartz) is similar to that of Mathinna Beds rocks from outside contact aureoles elsewhere in eastern Tasmania (*e.g.* Groves, 1977, p.16-17; Marshall, 1970, p.16-20, 69; Turner *in* McClenaghan *et al.*, 1982, p.14-15, 114). Such rocks display very low grade regional metamorphism, here diagnosed by the coexistence of chlorite with potash feldspar (Winkler, 1979, p.212, 219). There is no textural

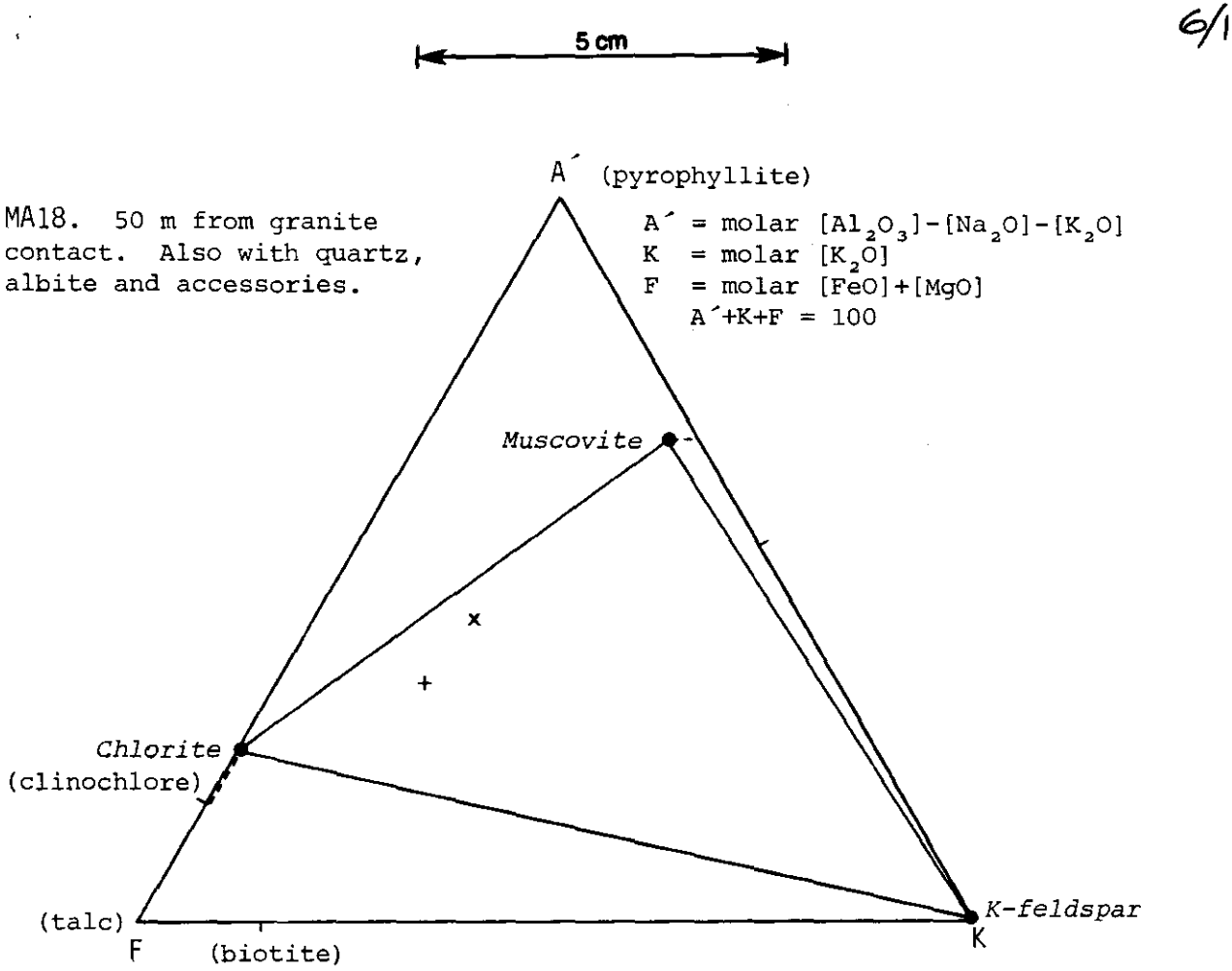

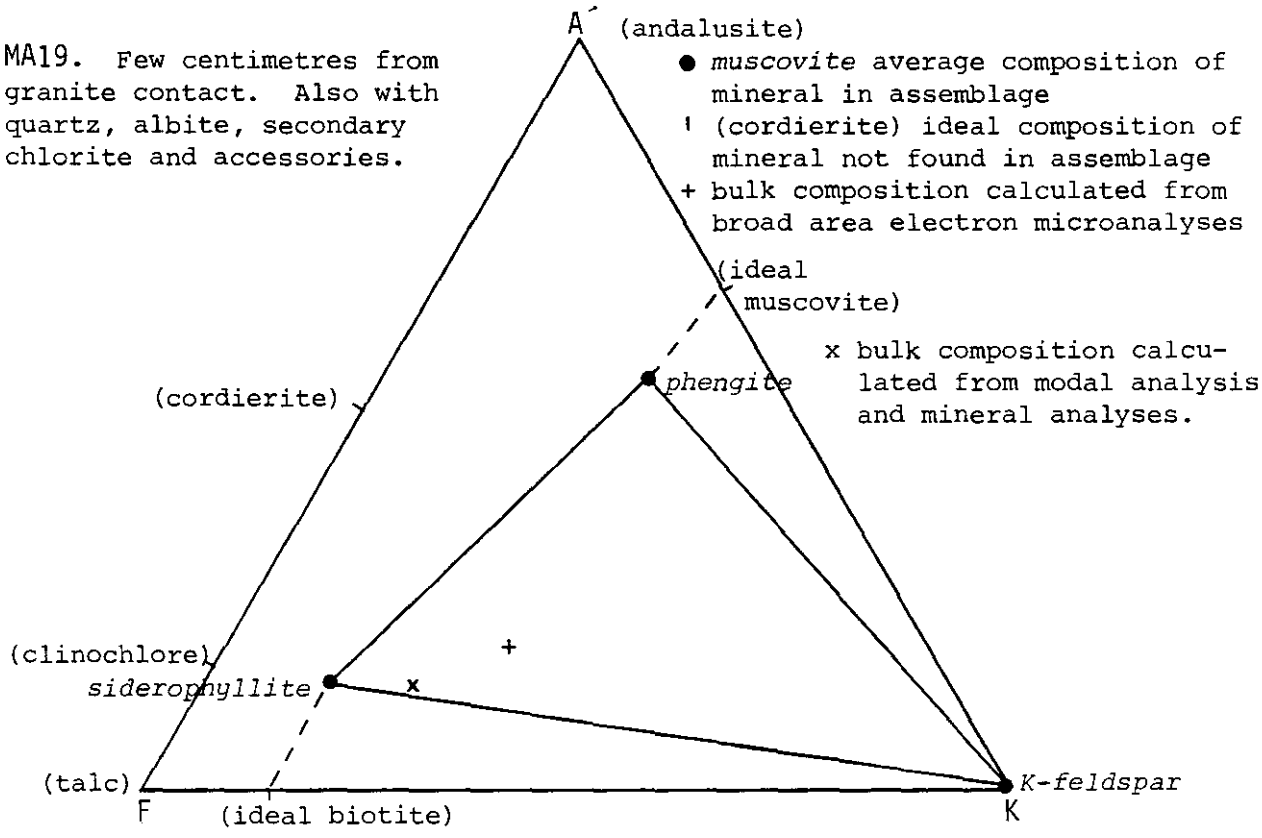

Figure 1. *Mineral compositions and assemblages of hornfels, plotted in A´FK diagrams.*

or compositional evidence in MA18 that chlorite is retrograde after earlier contact metamorphic biotite or other minerals, and the relative lack of recrystallisation is consistent with very low-grade metamorphism. The absence of biotite only 50 m from the granite contact seems unusual, although little petrological work has been done on the contact aureoles of the Devonian granites within the Mathinna Beds of eastern Tasmania.

In contrast, in sample MA19 from within a few centimetres of the contact, chlorite has disappeared and biotite formed, to give the assemblage: phengitic muscovite-biotite-K feldspar-albite-quartz.

The small amount of chlorite present is clearly retrograde after biotite and is compositionally different from the apparently prograde chlorite of MA18 (Tables 1, 2). A possible reaction producing biotite in these rocks is:

(1) $3(Mg,Fe)_5Al_2Si_3O_{10}(OH)_8+8KAlSi_3O_8 \rightleftharpoons 3KAl_2AlSi_3O_{10}(OH)_2+5K(Mg,Fe)_3AlSi_3O_{10}(OH)_2+9SiO_2+4H_2O$

The actual stoichometries would be slightly different as the minerals in MA18 and MA19 depart from their ideal compositions. Thermodynamic data from Helgelson *et al.* (1978) and Burnham *et al.* (1969) for the magnesium end-members suggest that ΔG is negative (*i.e.* clinochlore and K feldspar are incompatible) even at 1 bar (1×10^5Pa) and 25°C, but this is open to doubt, and data for iron-rich chlorites are not available. In any case, the reactions leading to the appearance of biotite in pelitic rocks are not well understood (*e.g.* Winkler, 1979, p.219), and it is possible that an intermediate phase such as stilpnomelane is involved.

MA19 has an unsuitable bulk composition, with a too low FeO/FeO+MgO and too high K_2O+Na_2O, for the development of chloritoid (which is incompatible with alkali feldspar) or staurolite, even if appropriate physical conditions were attained (Winkler, 1979, p.222). At the relatively low pressures of contact metamorphism, these rocks are probably also too magnesium-rich for the development of almandine garnet (Miyashiro, 1973, p.213). However, the bulk composition cannot account for the absence of cordierite, which is well known from contact metamorphosed Mathinna Beds elsewhere in eastern Tasmania (*e.g.* Groves, 1977, p.16-17; McNeil, 1965, p.39-41; Turner *in* McClenaghan *et al.*, 1982, p.119). Here two micas remain stable even at the contact, preventing the formation of the potash-feldspar-cordierite tie line (fig. 1). Thus the temperature at the contact was insufficient to produce rocks of the pyroxene-hornfels facies (termed the 'cordierite-K feldspar facies' by Winkler, 1967), and only the hornblende-hornfels facies was attained.

CONDITIONS OF METAMORPHISM

Some phase relations in the silica-saturated portion of the iron-free system K_2O-MgO-Al_2O_3-SiO_2-H_2O, are illustrated in Figure 2 (after Schreyer, 1976, p.312). The reaction

(2) $6KAl_2AlSi_3O_{10}(OH)_2+2KMg_3AlSi_3O_{10}(OH)_2+15SiO_2 \rightleftharpoons 3Mg_2Al_4Si_5O_{18}+8KAlSi_3O_8+8H_2O$

passes near the points (1kb, 520°C), (2kb, 575°C), 3kb, 620°C). Calculations based on the thermodynamic data of Helgelson *et al.* (1977) and Burnham *et al.* (1969) yield a slightly steeper equilibrium curve, with temperatures 10°-30°C higher. The effect of substitution of iron into phlogopite and cordierite is difficult to estimate, as a reliable internally

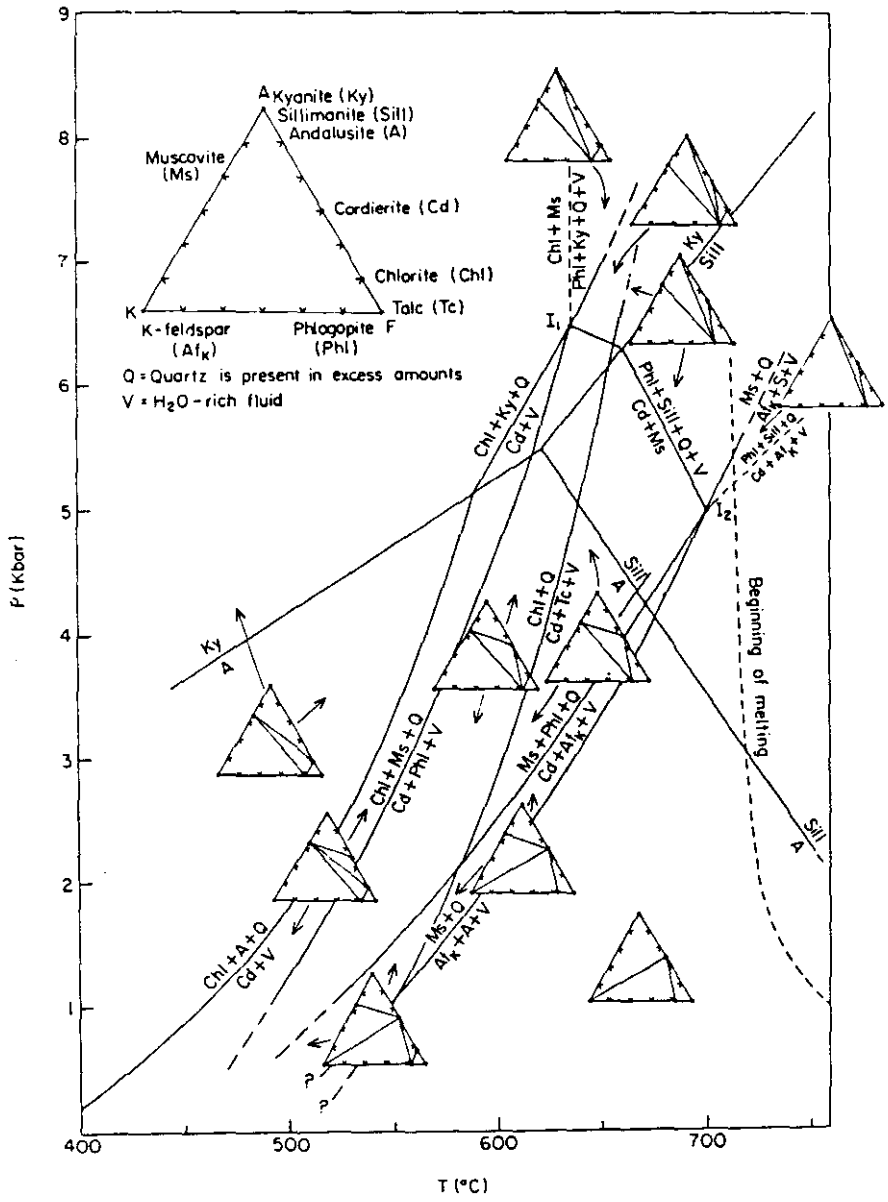

Figure 2. *Pressure-temperature diagram summarising the most important compatibility relations within the quartz-saturated portion of the system K_2O-MgO-Al_2O_3-SiO_2-H_2O at elevated temperatures and pressures between 0 and 7 Kbar based on the experimental work by Seifert (1970 and unpublished data). Except for quartz the crystalline phases involved in the reactions, and their abbreviations, are shown in the enlarged AKF-triangle (upper left) representing a projection of the H_2O- and SiO_2-saturated portion of the quinary system into a ternary subsystem Al_2O_3(=A)-K_2O Al_2O_3(=K)-MgO(=F) (from Schreyer, 1970, p.312).*

5 cm

consistent set of data including iron-cordierite (sekaninaite) does not seem to be available, but Schreyer (1965) concluded that the low temperature stability limit of Fe-cordierite was similar to that of Mg-cordierite. Another complication is the trioctahedral (phengitic) substitution into muscovite, and octahedral substitution into biotite in these rocks. This will probably stabilise the two-mica assemblage, shifting the equilibrium of (2) to higher temperatures.

Thus without further thermodynamic or experimental data it is not possible to accurately estimate a maximum temperature for the granite contact (MA19), even if the pressure is independently known. The most that can be said is that, assuming $P_{H_2O} \cong P_{total}$ = 1 to 2.5 kb, the temperature at the contact probably did not exceed 500° to 600°C, and was only a few hundred degrees 50 m away.

POSSIBLE IMPLICATIONS

Some possible explanations for the unusually narrow aureole and low temperatures at the contact are:

(*a*) the granitic intrusive may only be a small body. Field evidence is inconclusive, as the granite contact is close to and roughly parallel to the coast, and its eastern extent is unknown (see Clarke and Baillie, 1981).

(*b*) transfer of heat from the intrusive rock to the country rock was poor; for example the intrusive rock was relatively dry and $P_{H_2O} < P_{total}$, inhibiting convection. This is thought unlikely for a granitic intrusive.

(*c*) the granitic intrusive was intruded at a relatively low temperature. This seems the most likely explanation.

REFERENCES

BURNHAM, C.W.; HOLLOWAY, J.R.; DAVIS, N.F. 1969. Thermodynamic properties of water to 1000°C and 10,000 bars. *Spec.Pap.geol.Soc.Am.* 132.

CLARKE, M.J.; BAILLIE, P.W. 1981. Geological atlas 1:50 000 series. Sheet 77 (8512N). Maria. *Department of Mines, Tasmania.*

GROVES, D.I. 1977. The geology, geochemistry and mineralisation of the Blue Tier Batholith. *Bull.geol.Surv.Tasm.* 55.

HELGELSON, H.C.; DELANY, J.M.; NESBITT, H.W.; BIRD, D.K. 1978. Summary and critique of the thermodynamic properties of rock-forming minerals. *Am.J.Sci.* 278A.

HEY, M.H. 1954. A new review of the chlorites. *Mineral.Mag.* 30:277-292.

McCLENAGHAN, M.P.; TURNER, N.J.; BAILLIE, P.W.; BROWN, A.V.; WILLIAMS, P.R.; MOORE, W.R. 1982. Geology of the Ringarooma-Boobyalla area. *Bull.geol. Surv.Tasm.* 61.

McNEIL, R.D. 1965. The geology of the Mt Elephant-Piccaninny Point area, Tasmania. *Pap.Proc.R.Soc.Tasm.* 99:27-50.

MARSHALL, B. 1970. Geological atlas 1 mile series. Zone 7 sheet 31 (8315N). Pipers River. *Explan.Rep.geol.Surv.Tasm.*

MIYASHIRO, A. 1973. *Metamorphism and metamorphic rocks.* George Allen and Unwin Ltd : London.

SCHREYER, W. 1965. Zur stabilität des ferrocordierits. *Beitr.Mineralogie Petrographie* 11:297-322.

SCHREYER, W. 1976. Experimental metamorphic petrology at low pressures and high temperatures, *in* BAILEY, D.K.; MACDONALD, R. *The evolution of the crystalline rocks.* 261-331. Academic Press : London.

SPRY, A. 1969. *Metamorphic textures.* Pergamon Press : Oxford.

WINKLER, H.G.F. 1967. *Petrogenesis of metamorphic rocks. Second edition.* Springer-Verlag : New York.

WINKLER, H.G.F. 1979. *Petrogenesis of metamorphic rocks. Fifth edition.* Springer-Verlag : New York.

[26 April 1983]